GEOFIZIKA VOL. 25 No. 2 2008

Original scientific paper
UDC 551.510.42

A trajectory analysis of summertime ozone pollution in Slovenia

*Rahela Žabkar, Jože Rakovec and Saša Gaberšek**

University of Ljubljana, Faculty of Mathematics and Physics, Chair of Meteorology, Slovenia

Received 16 June 2008, in final form 3 November 2008

Annual number of days with exceeded ozone threshold values at the ground level measuring stations in Slovenia ranges from a few days in the interior of the country to up to 25 days at the Mediterranean stations. The highest number of ozone exceedances is usually recorded in the southwestern part of Slovenia, close to the Adriatic Sea, where favorable meteorological conditions enhance ozone formation. Local emission sources in this part of the country cannot explain the measured level of pollution. In addition, high ozone concentrations are occasionally measured at some Slovenian rural sites. We performed an ozone analysis with respect to air mass origin to provide an insight into processes leading to the high measured values of near-ground ozone. Three dimensional back trajectories were computed with a 3 hour-time interval for four measuring sites in Slovenia, generating eight arrival times per day starting at 00 UTC, for the warm parts (April – September) of the years 2003 and 2004. Trajectory clustering was used to determine typical pathways of air masses. Ozone and basic meteorological characteristics of trajectory clusters were further analyzed and multiple comparison tests were applied to determine which pairs of clusters differ significantly in measured ozone. In addition, concentration weighted trajectory (CWT) and number density (ND) of »polluted trajectories« were calculated to provide additional information about possible emission source regions.

Results suggest that high ozone concentrations appear most often in the short trajectory clusters of slow-moving air masses originated from SW. Moreover, CWT and ND fields confirm that high near-ground ozone levels in Slovenia are usually associated with trajectories originating from the area of the northern Adriatic Sea and its coastal regions. A heavily industrialized Po River Basin does not appear to have a significant direct impact on measured ozone concentrations in Slovenia, but may considerably contribute to the overall pollution over the northern Adriatic Sea together with coastal emissions.

Keywords: Tropospheric ozone, trajectories, clustering, transport

* Current Affiliation: UCAR/Visiting Scientist, Naval Research Laboratory, Monterey, CA, USA

1. Introduction

The photochemical pollution in southern Europe is severe during the warm part of the year. In Slovenia, the highest ozone concentrations occur in the southwestern part close to the Adriatic Sea, as well as in the urban areas in the interior of the country. The number of days with exceeded ozone threshold values in Slovenia during the warm part of the year varies from a few days for the capital city of Ljubljana, to up to 25 days with daily maxima over 180 $\mu g/m^3$ (warning hourly threshold value) for the Mediterranean stations. Measurements suggest that ozone concentrations close to the ground are high and the threshold values are exceeded also in the sparsely inhabited rural areas all over Slovenia. This implies that transport of polluted air masses, which is the subject of the present paper, has an important effect on the photochemical pollution.

Transport of air masses to the regional air quality station Mt. Krvavec (WMO-GAW station in Slovenia) has been studied within Vertical Ozone Transports in the Alps Projects (VOTALP, VOTALP II; Wotawa and Kromp-Kolb, 2000). In the scope of these and some other projects the Po Basin was identified as the important source region of Alpine ozone precursors (Prevot et al., 1997; Seibert et al., 1997; Wotawa et al., 2000; Kaiser et al., 2007). Characteristics of ozone seasonal and diurnal variations at Mt. Krvavec were also investigated by Scheel et al. (1997) and Bizjak et al. (1999), while local ozone characteristics at Slovenian rural sites have been studied by Gomišček et al. (1996, 1997a, 1997b).

The conclusions of Seibert et al. (1997), Wotawa et al. (2000) and Kaiser et al. (2007) analyzing Mt. Krvavec lead to the following question: Do the Po Basin emissions have significant impact on ozone concentrations also in other parts of Slovenia, especially in the southwestern part with the highest measured occurrence of the exceeding ozone concentrations? For urbanized areas, like the capital city of Ljubljana, the assumption is that high ozone concentrations occur mainly due to local emissions of primary pollutants. With no significant local emission sources close to a rural measuring station in Iskrba, the transport of polluted air masses might play a dominant role, but contributions of relatively nearby urban plumes and the long-range transport of ozone rich air to this site remain to be investigated.

Four observation sites were selected in order to assess ozone pollution over Slovenia. Three-dimensional backward trajectories were calculated, based on meteorological fields with relatively high spatial and temporal resolution of 9.5 km and 1 hour, respectively. The resolution was considerably higher than in previous related studies (Seibert et al., 1997; Kaiser et al., 2007; Cristofanelli et al., 2007; Riccio et al., 2007; Galvez, 2007). For example Seibert et al. (1997) used three different types of back trajectories, the highest resolution trajectories were calculated on the basis of ECMWF fields with a horizontal resolution 0.5° and temporal resolution 3 hours. Cristofanelli et al. (2007) and Kaiser et al. (2007) used ECMWF meteorological fields with 1.0° horizontal resolution, while Riccio et al. (2007) calculated trajectories on NCEP/NCAR re-analysis with 2.5°

spatial resolution and temporal resolution of 6 hours. The high resolution of the trajectories in our research is vital because of a very complex topography in this part of Europe and because we are investigating the origin of the polluted air masses for low altitude measuring sites. Both the regional transport from remote emission areas as well as relatively nearby urban plumes (up to 50 km distant) can influence the measured ozone concentrations at these stations.

Trajectory analysis consisted of two parts. In the first part we classified the trajectories into groups of similar trajectories, using the *k*-means trajectory clustering procedure. We analyzed inter-cluster variations of measured ozone concentrations and basic meteorological parameters at the receptor sites. In the second part, concentration-weighted trajectories (CWT, Seibert et al., 1994) in combination with number density (ND) of »polluted trajectories« (i.e. trajectories with high measured ozone at receptor points) were applied to identify the locations of potential pollution sources. The CWT method distributes the ozone concentration along the trajectories evenly and is able to distinguish major sources from moderate ones by calculating concentration gradients. ND results represent potential source directions rather than locations. In addition, the trailing effect, where areas upwind and/or downwind of receptor point are likely to be identified as sources as well, must be taken into account. Thus, combining the two methods yields better information about the source areas.

2. Methodology

2.1. Selected locations and their ozone characteristics

Among the 18 ground level stations in Slovenia with continuous ozone measurements, the stations at Nova Gorica (suburban), Ljubljana (urban), Mt. Krvavec and Iskrba (both rural) were selected for a detailed analysis (Table 1, Figure 1). The stations are not under the influence of direct emission sources and are considered to be representative for ozone concentrations in their surroundings.

Nova Gorica (NG) at the border with Italy is the westernmost station with a Mediterranean climate. Hot summers with a low number of precipitation days promote photochemical ozone production. The exceeded ozone concentrations are the most frequent of all the sites: altogether 162 hours with ozone concentration above 180 $\mu g/m^3$ were measured in the years 2003 – 2005. There are some moderate local emission sources in the vicinity, mainly from traffic. Major potential sources are located within a radius of about 40 km (i.e. Udine, Monfalcone, Trieste).

Ljubljana (LJ), the capital of Slovenia, represents the urban ozone case. The population of Ljubljana is about 300.000 and the city is located in a basin (over 20 km W-E by some 40 km N-S). There were altogether 33 hours with ozone concentration exceeding 180 $\mu g/m^3$ in the years 2003 –2005. The direct impact of nearby emissions on the measured ozone is relatively weak except

Table 1. Selected monitoring stations. Beside the exact coordinates of the stations, also the coordinates of the final trajectory points including the height of the model topography for these points are shown.

Monitoring station	Abbr.	Height (m)	φ (°N)	λ (°E)	Height $_{traj}$ (m)	φ_{traj} (°N)	λ_{traj} (°E)	Type of station and type of zone
Nova Gorica	NG	55	45.90	13.63	110	45.83	13.55	Background suburban
Ljubljana	LJ	298	46.06	14.52	333	46.11	14.52	Background urban
Krvavec	KV	1710	46.23	14.53	1353	46.35	14.60	Background rural (regional)
Iskrba	IS	540	45.56	14.86	541	45.55	14.86	Background rural (regional)

during the rush hour. The measured ozone concentrations are supposed to be representative for the Ljubljana region.

Mt. Krvavec (KV) is located on the foothills of the eastern Alps within the Alpine climate zone. The site is situated about 30 km north of Ljubljana and lies on a ridge surrounded by peaks between 1500 and 2500 meters above sea level. Threshold values are occasionally exceeded: 23 hours with ozone above 180 μg/m^3 in the years 2003 – 2005. High average ozone concentrations are due to the absence of nighttime ozone removal, which is more important at the lower altitude stations (Figure 2), and is typical for a site located above the stable nocturnal boundary layer (Scheel et al., 1997). KV has already been studied by Kaiser et al. (2007), but we decided to include it in our study with

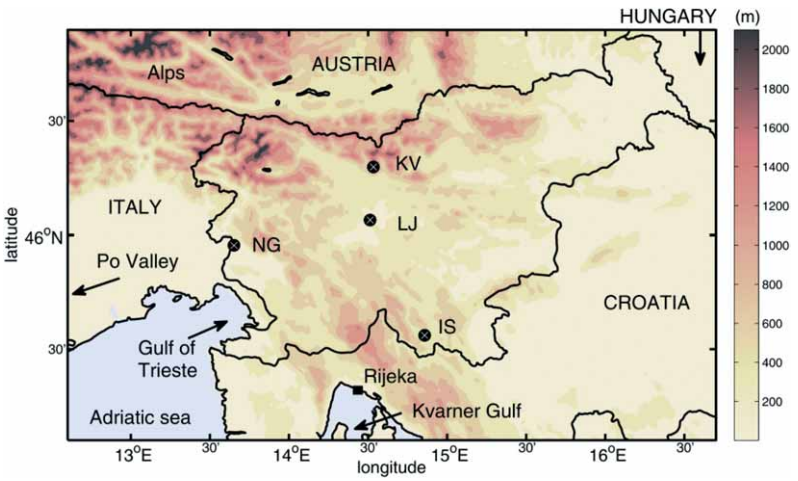

Figure 1. Orography of Slovenia at 1 km resolution and locations of selected ozone measuring sites.

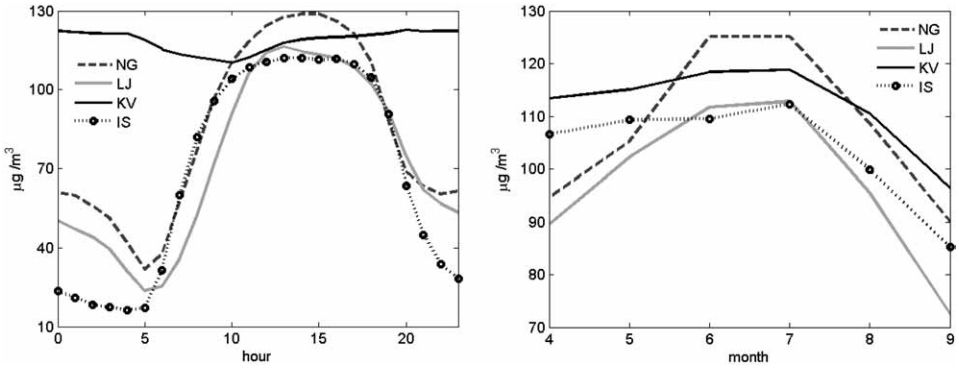

Figure 2. Left: Average daily variations of ozone concentration at Nova Gorica (NG), Ljubljana (LJ), Krvavec (KV) and Iskrba (IS) for the months June and July from 2003 to 2006. Hours represent UTC. Right: Average monthly values for the warm period of the years 2003 to 2006. For NG, LJ and IS average monthly values were calculated based on the daytime ozone (hourly values from 11 to 17 UTC were considered), while for KV hourly concentrations throughout the day were taken into account.

higher spatial and temporal resolution of meteorological fields and different methods used for trajectory analysis.

Iskrba (IS) is located on a plateau, in a grassy glade, surrounded by forest with predominantly coniferous trees covering the hills and mountains at an altitude of approximately 800 – 1200 meters. The rest is grassland (not grazed by domestic animals) and partly also farmed (grass, pasture). Occasional high-level ozone concentrations measured at this rural background station (16 hours above 180 $\mu g/m^3$ in 2003 – 2005) suggest advection of polluted air. Major potential source emission areas are at least 40 km away, such as Rijeka (Croatia, 40 km to the southwest) or Ljubljana (50 km to the northwest), while the highly industrialized Italian cities in the west are rather distant.

The first insight into the ozone concentration statistics is provided by average daily and seasonal ozone concentrations for the four stations (Figure 2). For stations at lower altitudes (LJ, NG, IS) the diurnal ozone cycles are very pronounced. Daily maxima in the hottest months (June and July) are on average the highest at NG, which is a consequence of both polluted air and very favorable weather conditions for ozone formation. Differences in daily maxima between LJ (urban) and IS (rural) are negligible during these months, which is a surprising finding. To some extent this could be due to local emissions in Ljubljana resulting in somewhat lower measured ozone values. Nevertheless, the measured ozone concentrations in Iskrba are unusually high and require further explanation. Nighttime ozone minima for the three stations can be explained by the nocturnal destruction by NO_x scavenging and dry deposition. A comparison of average nighttime ozone values shows the highest ozone reduction for IS and the lowest for NG, with the LJ curve being similar to NG. The very effective ozone destruction in IS can be explained by the formation of sta-

ble nighttime boundary layer above the glade, where the measurement site is located. Dry deposition and local biogenic NO soil emissions, produced by microorganisms and bacteria in the nearby conifer forests (Pilegaard, 2006), in coincidence with the suppressed vertical mixing deplete the ozone in the near the ground layer. The amount of local biogenic NO emissions are small but sufficient, because of inefficient ozone replenishment from the boundary layer due to the reduced vertical mixing. Effective dry deposition of ozone as well as other pollutants is a consequence of the higher surface roughness and the surface area of the forest. The nighttime air mixing over town (LJ and NG) is not entirely suppressed and the nocturnal emissions are only due to rare traffic, resulting in higher nighttime ozone concentrations at these stations. In addition, typical local diurnal circulations develop during the calm weather conditions associated with highest daily ozone maxima. Consequently, ozone formed during the day, and transported outside the urban areas toward surrounding hills by daytime winds, slowly drains back during the night, resulting in slightly higher nocturnal ozone concentrations. Distinct minima at about 5:00 UTC are caused by the morning rush hour (note that 5:00 UTC = 7:00 CEST).

The KV site lies above the boundary layer at night and sometimes even during the day, with the ozone concentrations less susceptible to local emissions. The diurnal ozone cycle at KV is typical for a higher mountain stations and similar to the lower free troposphere variations (e.g. Balzhanov, 1994; Scheel et al., 1997). A slight minimum at about 10:00 UTC corresponds to the time when the well-mixed layer reaches the station, causing an ozone decrease due to the arrival of fresh locally polluted air.

For the comparison of monthly variations (right panel in Figure 2) only hourly values from 11:00 to 17:00 UTC were taken into account to eliminate an impact of the nighttime ozone removal for the three low level stations. For KV all hourly values were considered. Both regional rural stations (KV and IS) are characterized by relatively high ozone levels in the spring, almost comparable to the summer time maxima. The high spring ozone levels have been extensively studied and the conclusions of different studies were reviewed by Monks (2000), who concluded there was still no consensus on the formation mechanisms. We speculate that high concentrations in spring are due to the winter accumulation of precursors, causing high ozone concentrations with the onset of favorable springtime weather conditions. The two stations (LJ, NG) exhibit distinct summer maxima, associated with the photochemical production of ozone from VOCs and NO_x under the influence of intensive solar radiation at polluted sites (e.g. Lefohn et al., 1992; Derwent and Davies, 1994; Logan, 1985, 1989; Scheel et al., 1997).

2.2. Trajectories

The meteorological fields used for trajectory calculations were computed with ALADIN/SI model (ALADIN IT, 2003). The spatial domain spanned from

2 W to 28 W and from 36 N to 54 N. The horizontal resolution was 9.5 km and 37 vertical levels extended from the ground to the 5 hPa level. The temporal resolution of wind fields used for trajectory calculations was 1 hour. Three-dimensional backward trajectories were then calculated by using the FLEXTRA trajectory model (Stohl et. al., 1995; Stohl and Seibert, 1998) for arrival levels 50 meters above the model topography. Each trajectory calculation started 96 hours prior to the arrival time. Their positions were stored at one-hour time intervals. The coordinates of final trajectory points were slightly shifted with respect to the true measuring site locations, as evident from Table 1. Hence, the final trajectory points do not match the exact geographical measuring site coordinates (latitude, longitude), but they better meet the true local relief characteristics of the measuring site in the coarse model topography (e.g., if the measuring site is located on the southern slope of the hill, then the final trajectory point was placed on the southern slope of this hill, as it is resolved by the model topography). Trajectories were calculated for eight arrival times per day (00, 03,..., 21 UTC) for the warm periods (months from April to September) of 2003 and 2004.

2.3. The k-means clustering

To aggregate trajectories into groups with similar characteristics the *k*-means clustering algorithm was applied (Moody and Galloway, 1988). This method was used also for trajectory clustering to determine potential source regions (Mahura et al., 1999; Cape et al., 2000; Lin et al., 2001; Abdalmogith and Harrison, 2005; Sanchez-Ccoyllo et al., 2006; Hafner et al., 2007), for studying the synoptic patterns (Avila and Alarcon, 1999; Seibert et al., 2007), or different air quality regimes (Flemming et al., 2005; Kim Oanh et al., 2005; Makra et al., 2006).

The *k*-means clustering algorithm iteratively allocates the set of N objects (trajectories in our case) among a predetermined number of clusters k, until the sum of distances from each object to its cluster centroid over all clusters cannot be decreased any further. Before the algorithm is initialized, the k initial cluster centroids (seeds) must be defined. Since the procedure is only guaranteed to converge to a local solution, which can significantly differ from the global one, the initial selection of seeds might significantly impact the classification (e.g. Pena et al., 1999; Groenen and Jajuga, 2001). Our strategy concerning this issue was to use the »multiple random starts« procedure, where the initial seeds were randomly selected k trajectories from total. The clustering procedure was then repeated many (800) times and among the obtained results the one with the minimum sum of distances of all trajectories from its cluster centroids was selected and used in further analysis. For clustering purposes only the last 24 hours of each trajectory were considered because a significant amount of longer trajectories (48 hours and longer) escaped out of the domain and could not be used. The Euclidean distance between trajectories $\boldsymbol{x_i}$

and $\boldsymbol{x_j}$ was calculated at 24 points l as $d^2(\boldsymbol{x_i},\boldsymbol{y_i}) = \Sigma_l\{(x_{li} - x_{lj})^2 + (y_{li} - y_{lj})^2\}$, where (x_{li}, y_{li}) were the coordinates of trajectory $\boldsymbol{x_i}$ at a point l. No data measured at the arrival point was considered in the clustering process. We decided not to explicitly include altitude of the trajectory points in the distance calculations. It is actually built-in implicitly because winds tend to be faster at higher altitudes, thus longer trajectories tend to be associated with higher altitudes. A similar approach was also used by some other authors (Owen, 2003; Harris et al., 2005; Hafner et al., 2007).

The final number of clusters was then determined as follows. The aim was to choose and analyze a stable and objective clustering solution, representing true main pathways, i.e. the solution which does not change considerably by adding or eliminating trajectories. The silhouette coefficient (SC) (Rousseaw, 1987), a dimensionless measure of both internal cluster cohesion and external cluster separation (Figure 3), was used in selecting the most appropriate number of clusters k. The first step in calculating SC is the computation of silhouette $S(i)$ for each i-th trajectory by the following equation:

$$S(i) = \frac{b(i) - a(i)}{Max(a(i), b(i))}.$$

If i is classified into cluster A, then $a(i)$ is an average dissimilarity of i to all other objects in A, and $b(i)$ is an average dissimilarity of i to all objects in neighboring clusters B. $S(i)$ ranges between –1 and +1, where a silhouette value close to +1 indicates that an object has been well classified, while a value close to –1 implies that an object has been misclassified. The average value of S across all objects is called a Silhouette Coefficient (SC), which summarizes how well the cluster structure fits the data.

The SC course for four sites is shown in Figure 3. In general the SC value unevenly decreases with the number of clusters k. The tendency was to choose the classifications with as high SC value as possible. At the same time, since the parameter k controls the resolution of the clustering solution (increasing k generates solution with smaller and more compact clusters), the number of total clusters must be sufficiently high for the needs of the further ozone analysis. For LJ the choice of trajectory classification into 7 clusters was natural (see Figure 3), while for KV and IS the classification into 6 clusters overcome the 7 clustering solution according to SC value. For NG the selection of classification with 7 clusters was rather subjective – there are only slight differences in SC between solutions with 6 and 8 clusters. Nevertheless, the ozone analysis performed for solutions with 6 and 8 clusters (not presented in the paper) lead to similar conclusions as the 7 clustering solution, presented below.

2.4. Analysis of cluster parameters

Hourly values of measured meteorological parameters (temperature, relative humidity and precipitation) and ozone concentrations at the time of ar-

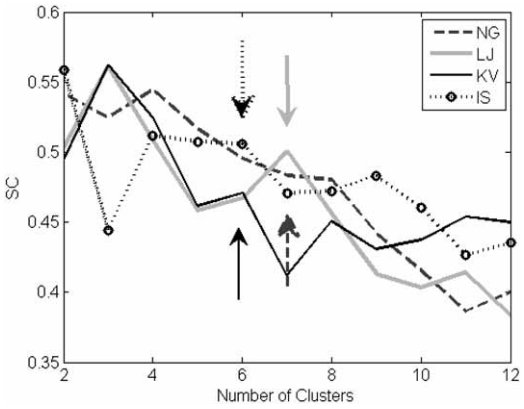

Figure 3. Silhouette coefficient for the first stage clustering of trajectories for all the stations. Arrows denote selected number of clusters, used in further analysis.

rival at the trajectory destination points were assigned to each computed trajectory. The measured data was provided by the Environmental Agency of the Republic of Slovenia. Values of these parameters were analyzed for each trajectory cluster. Tukey's least significant difference (LSD) multiple comparison procedure (Hochberg, 1987) and Kruskal-Wallis test (Hollander and Wolfe, 1973; Gibbons, 1985) were then used for the pair wise comparisons of average cluster values to determine clusters that significantly differ in these parameters, particularly in ozone. LSD procedure is a simple *t*-test, while Kruskal-Wallis test is a nonparametric version of the classical one-way ANOVA, which does not assume a-priori a normal distribution of data. Another characteristic of the Kruskal-Wallis test is smaller sensitivity to outliers. The ranks in the Kruskal-Wallis test are obtained by sorting all the cluster values (e.g. ozone concentrations) into ascending order and then calculating mean rank of concentrations for each cluster.

2.5. Concentration-weighted trajectory (CWT)

A method of weighting trajectories with associated concentrations was introduced by Seibert et al. (1994) and its results were compared to other trajectory statistical methods by e.g. Ying-Kuang Hsu et al. (2003) and Scheinfinger and Kaiser (2007). In this procedure, each grid cell is assigned a concentration obtained by averaging trajectory-associated concentrations that had crossed the grid cell:

$$C_{ij} = \frac{1}{\sum_{k=1}^{N} n_{ijk}} \sum_{k=1}^{N} C_k n_{ijk}.$$

C_{ij} is weighted concentration in the (i,j) grid cell, C_k is concentration of k-th trajectory at the receptor point, N is the total number of trajectory endpoints in (i,j) grid, and n_{ijk} is the number of k-th trajectory endpoints in the (i,j) grid cell. The denominator corresponds to (i,j) grid cell number density ND_{ij}.

3. Results and discussion

3.1. The trajectory clusters and local ozone concentrations

The average cluster trajectories for stations NG, LJ, KV and IS are presented in Figure 4. The influence of the Alpine barrier dictates the main airflow characteristics. There are two dominant paths of air masses reaching Slovenia: from the SW and from the NE. The trajectories from these two main directions are initially disaggregated with respect to the trajectory lengths, resulting in one cluster of slow and short trajectories originating from the NE and one from the SW. The long and fast moving trajectories are further disaggregated into groups originating from more distant westerly and easterly areas. There are generally two long trajectory clusters with low altitudes, one from the SSE and the other from the SW. Longer trajectories from the N are further split into a cluster east of the Alps over Eastern Austria and a cluster (or two) descending over the Alps from the NW. A slightly different overall cluster distribution for KV (Figure 4) is due to the reduced orographic effect on the higher altitude of the measuring station.

Basic characteristics of air masses approaching the measuring sites (in correspondence to the trajectory clusters) are summarized in Table 2, including ozone concentration, air temperature, relative humidity and precipitation. Clusters are uniformly labeled for all the stations and they generally follow the cluster average ozone maximum: clusters 1 of short trajectories from SW with the highest maximum, followed by cluster 2 of (again short) trajectories from NW, etc. Cluster 7 of long trajectories across the Alps is the one with the lowest maximum.

In addition to the air mass origin, the prevalent local meteorological conditions associated with a specific cluster also play an important role in the ozone pollution. Some basic characteristics of the average cluster meteorological parameters can be deduced from Table 2. For clusters with average values that significantly differ in the value of the variable at significance level 0.05 (according to the LSD multiple comparisons), the numbers are emphasized in bold. Air masses, originating from the north and crossing the Alps, are usually associated with the significantly lower temperatures at the sites (e.g. clusters 7 and 5). The percentage of precipitation days is higher in clusters of trajectories originating from the south, associated with the Mediterranean cyclone. High temperatures are generally positively correlated with the ozone formation – the correlation coefficient between ozone and temperature daily maxima is 0.75, 0.82, 0.47, 0.74 for NG, LJ, KV and IS, respectively. The average

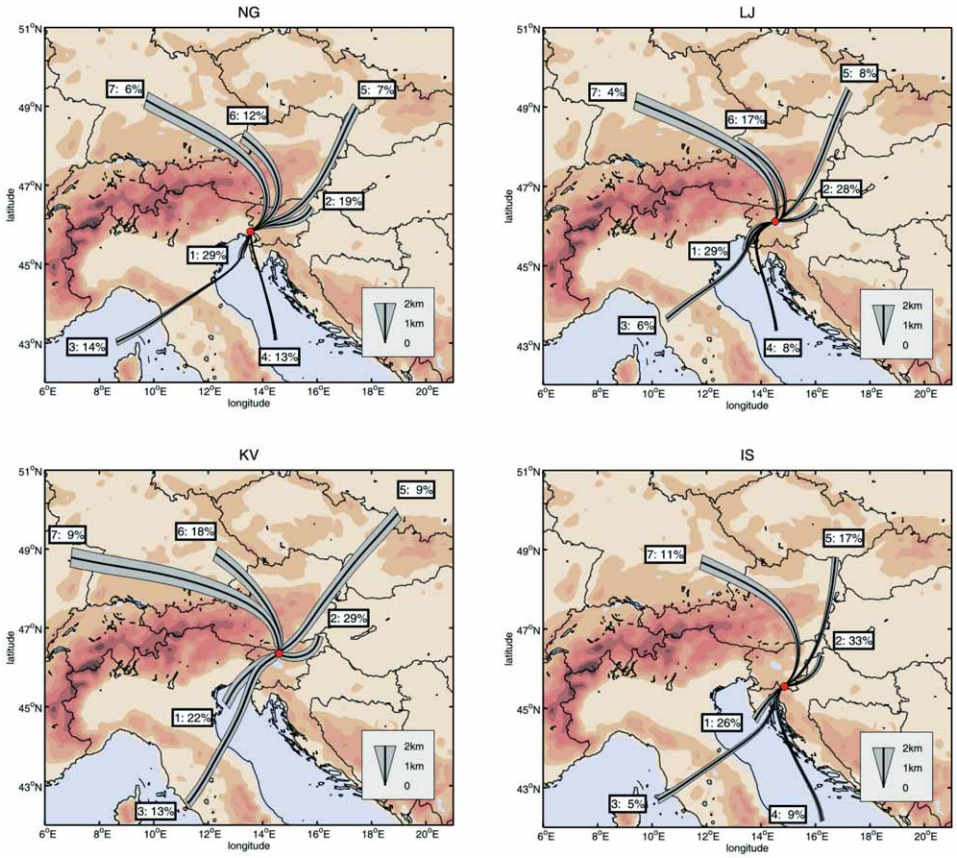

Figure 4. Average cluster trajectories for Nova Gorica (NG), Ljubljana (LJ), Krvavec (KV) and Iskrba (IS). Text boxes denote the cluster number and the percentage of trajectories involved in cluster. Path widths measure average above ground level (AGL) of cluster trajectories. ALADIN topography (resolution 9.5 km) above 500 m AMSL, with the contour intervals 500 m are shown in the background.

relative humidity (RH) has in our case no evident impact on the ozone. This is partly due to different reasons for high and low humidity values. For example, the highest RH in cluster 7 for LJ is mainly associated with very low temperatures in this cluster, while for KV high RH in cluster 2 stems from air moistening above the Adriatic Sea. The correlation coefficients between daily ozone maxima and daily RH minima are now –0.5, –0.63, –0.45 and –0.70 for NG, LJ, KV and IS, respectively. Like RH, the precipitation enabling wet deposition of air pollutants is negatively correlated to measured ozone.

Figure 5 shows characteristics of the 3-hourly ozone maxima associated with the cluster trajectories arriving at 12:00 and 15:00 UTC to NG, LJ and IS. Including all trajectories and associated ozone values for the three stations

Table 2. Number of trajectories, meteorological parameters and ozone concentrations for stations NG, LJ, KV and IS associated with clusters in Figure 4. Ozone (O3), temperature (T) and relative humidity (RH) are averaged over all trajectories, regardless of the time of arrival. Daily maxima are assigned to the trajectories arriving at 12:00 and 15:00 UTC and then averaged over all cluster 12:00 and 15:00 UTC trajectories. Ozone daily minima are assigned to and averaged over the 6:00 UTC trajectories, while accumulated daily precipitation (RR) was assigned to all cluster 12:00 UTC trajectories. Significantly different average values (t-test, 0.05 significance level) are written in bold style.

Cluster	*N*	O_3 (g/m^3)	O_3 max (g/m^3)	O_3 min (g/m^3)	*T* (C)	*T*max (C)	*RH* (%)	*RR* (mm)*
NG: O_3(annual) = 51 g/m^3								
1	923	75.0	**140.9[a]**	18.8	20.2	27.6	64.5	7 (21/5)
2	570	74.6	128.9	22.0	22.1	**29.2[a]**	59.6	5 (10/–)
3	277	**86.3[a]**	130.1	23.5	21.4	26.5	66.2	17 (20/6)
4	373	72.9	125.2	16.9	19.6	25.4	69.5	12 (12/2)
5	236	75.9	109.2	31.5	19.9	25.7	**51.3[c]**	5 (4/–)
6	308	67.7	107.8	26.7	19.6	25.9	56.9	11 (10/2)
7	218	**58.3[c]**	**92.6[c]**	21.1	**15.2[c]**	**21.5[c]**	59.7	9 (9/2)
LJ: O_3(annual) = 45 g/m^3								
1	744	69.4	**127.3[a]**	14.0	19.3	25.6	68.1	13.5 (35/9)
2	824	60.4	114.9	13.3	18.8	24.6	71.9	11.1 (22/3)
3	211	**77.0[a]**	107.5	22.6	17.8	22.5	70.0	17.3 (8/3)
4	231	**78.9[a]**	117.8	23.0	18.3	23.5	70.3	18.0 (14/5)
5	264	56.1	106.8	10.8	**15.4[d]**	21.8	69.1	4.0 (5/–)
6	434	58.9	101.1	16.8	17.4	22.3	70.2	12.8 (16/4)
7	196	**39. 5[c]**	**77.1[c]**	10.4	**10.7[c]**	**14.2[c]**	**81.0[a]**	9.8 (5/1)
KV: O_3(annual) = 99 g/m^3								
1	638	**123.4[a]**	**136.7[a]**	**105.5[a]**	11.2	15.0	75.5	17.0(39/11)
2	834	116.3	128.1	100.3	12.1	16.6	77.5	9.6 (33/4)
3	359	116.0	125.4	98.0	8.8	11.8	**87.8[a]**	13.3 (17/4)
5	254	113.0	120.5	100.7	**6.5[d]**	10.5	80.8	3.6 (6/–)
6	528	**105.3[d]**	115.3	92.4	8.7	12.4	78.3	8.8 (21/3)
7	252	**96.3[c]**	**103.7[c]**	**83.8[c]**	**5.4[c]**	**8.1[c]**	80.3	8.4 (9/1)
IS: O_3(annual) = 57 g/m^3								
1	802	63.9	**128.7[a]**	7.6	15.3	23.9	73.6	11.3 (28/6)
2	895	59.6	115.2	6.8	15.8	23.4	74.0	11.3 (24/2)
3	185	**83.7[b]**	115.0	27.4	15.6	20.4	74.4	16.9 (13/4)
4	288	**84.7[b]**	121.0	**41.0[a]**	15.5	21.7	73.7	14.3 (13/5)
5	439	65.7	107.1	13.8	13.3	19.0	76.4	7.9 (19/1)
7	298	61.7	**96.4[c]**	16.3	**10.8[c]**	**16.4[c]**	77.7	13.0 (13/3)

* (a/b) is precipitation frequency in days, a – above 1 mm, b – above 20 mm
[a] average cluster value significantly higher than any other average cluster value
[b] average cluster value significantly higher than any except one average cluster value
[c] average cluster value significantly lower than any other average cluster value
[d] average cluster value significantly lower than any except one average cluster value

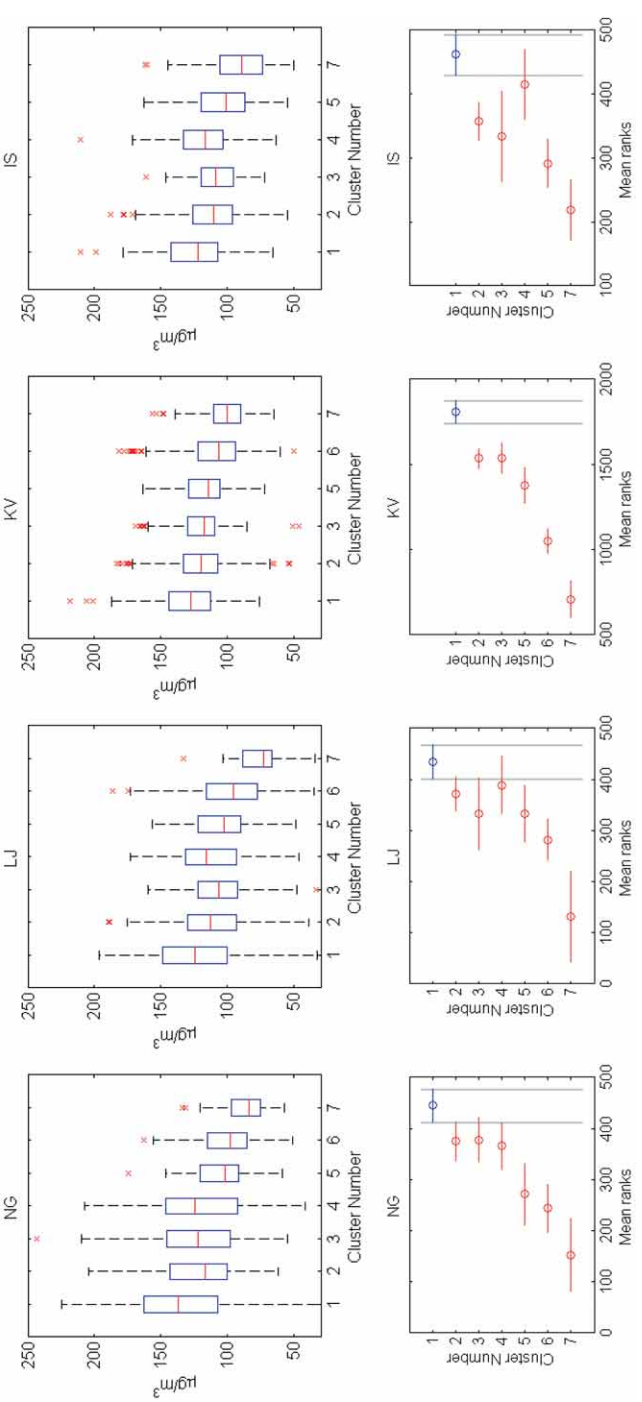

Figure 5. Analysis of average cluster ozone mixing ratios for NG, LJ, KV and IS, cluster centroids are shown in Figure 4. Upper panel: box-and-whisker plots of the 3 hourly ozone maximum associated with trajectories arriving at 12:00 and 15:00 UTC for sites NG, LJ and IS; for KV all trajectories are taken into account. Boxes extend from the lower quartile, over median to the upper quartile values. The whiskers specify 1.5 times the interquartile range and crosses beyond the whiskers represent outliers. Lower panel: mean ranks of Kruskall-Wallis test for the same data sets.

would result in lower average ozone concentrations due to nighttime ozone reduction. For KV without a pronounced daily cycle all cluster trajectories with associated 3-hourly ozone maximum were taken into account. For example, the 3-hourly maximum ozone data for 12 UTC includes maximum hourly values from 11:00 to 13:00 UTC. Box-and-whisker plots are presented in the upper panel of Figure 5, and the Kruskal-Wallis test results for the null hypothesis that ozone concentrations from any two clusters come from distributions with equal median (at 0.05 significance level) are shown in the lower panel of Figure 5.

For the pairs of clusters with non-overlapping ranks, the difference in medians of ozone concentrations is significant at 0.05 level. The daily maxima in Table 2 are for all stations associated with cluster of short trajectories from the SW. These clusters include stagnant anticyclone situations with light winds, highest daily temperatures and high solar irradinace, which are the most favorable situations for ozone formation. Note that ozone concentrations in short clusters from the NE with similar local meteorological conditions, sometimes on average even more favorable for ozone formation (higher average temperatures and less precipitation days), have maximum ozone concentrations slightly lower than those from the SW. Moreover, the differences between these two clusters (#1 and #2) are significant for all measuring sites according to *t*-test results for maximum ozone concentrations (numbers in bold style in Table 2) and for the three measuring sites (except LJ) according to Kruskal-Wallis test results for 3 hourly maximum (Figure 5 lower panel). Since cluster 2 has the highest ozone from all northern clusters, the difference between the short SW cluster and all northern clusters is significant. The difference between the short SW cluster and long southern clusters are usually not significant according to the Kruskal-Wallis test (NG cluster 3, LJ and IS cluster 4). Ozone concentrations associated with cluster 7 significantly differ from all the other clusters for all the stations regardless of the statistical test applied. Cluster 7 of long trajectories from NW across the Alps is thus the cluster with lowest ozone concentrations. The ozone in other long northern clusters is also low. This is due to the low temperatures (northern flow) and strong winds (long trajectories) that prevent efficient ozone formation. Since prevalent meteorological conditions in these clusters are unsuitable for effective ozone formation, meteorological conditions rather than air mass origins explain low ozone concentrations.

Cluster 1 for NG and LJ (left panels in Figure 6 and Table 2) with the highest daily maxima is associated with the lowest night time ozone values with a distinctive minimum at 6 UTC due to local NO traffic emissions (rush hour). Distinct minima at 6 UTC for these stations occur in all clusters. The lack of a distinctive minimum in IS, similar to Figure 2, is the consequence of different nocturnal ozone removal characteristics (see explanation in Section 2.1). The short clusters from SW with highest daily ozone maxima for the three low elevation stations exhibit very low daily ozone minima (Table 2 and left panels in

Figure 6). Short trajectories imply low wind speeds and poor mixing, so that dry deposition and local biogenic NO emissions from soil deplete the surface (measurement) layer faster than ozone can be transported downwards from the boundary layer. The opposite is true for KV, where the cluster with the highest daily ozone maximum also exhibits the highest daily minimum (and vice versa). This is due to the absence of a direct impact of local emissions and of reduced impact of the planetary boundary layer due to the station's elevation.

An interesting cluster (#4) for the remote station IS (low trajectories along the Adriatic Sea), has the second highest daily ozone maximum and also significantly higher daily ozone minimum. This cluster represents »old« polluted air masses (since the ozone in the air masses is due to »old« rather than »in situ« production, these air masses are usually called »old« polluted air masses). Stronger winds in this cluster prevent the formation of the stable nighttime inversion layer. Consequently, increased vertical mixing enable the ozone replenishment from the boundary layer. In such circumstances dry deposition and reactions with biogenic NO cannot deplete ozone in the near ground air, where the measurements are conducted. Measured ozone associated with these air masses thus conserves its relatively high level. A similar cluster for NG (cluster 4) has almost the same average ozone maximum, but much lower minimum, indicating there are more local emission areas upwind of NG. Clusters with relatively higher midnight ozone levels are beside IS (#3 and #4), NG (#5, long northerly trajectories), LJ (#3 and #4 long southerly trajectories) and KV (#1). Apparently, no common cluster of higher midnight ozone exists, suggesting that nighttime ozone removal depends on local site characteristics. But except for NG the highest nighttime ozone levels are associated with one of the southern clusters.

Monthly variations (right panels in Figure 6) are in general agreement with the results presented so far. The highest and the lowest ozone values appear with the same clusters as before. The highest ozone concentrations are measured during the hottest months. A closer look at intra-cluster variations reveals a rather unexpected leap in August for clusters approaching from the north (clusters 2, 5, 6). The August increase occurs in all northern clusters, the exception is only a group of clean trajectories crossing the Alps (cluster 7). The explanation of this phenomenon lies in a very hot August 2003, when an intense heat-wave affected Europe. Highly stable, hot and dry meteorological conditions (Schaer et al., 2004; Black et al., 2004), resulted in high ozone concentrations measured all over Europe (Vautard et al., 2005; Ordonez et al., 2005). In August 2003 very high ozone concentrations were measured in Slovenia between 4th and 15th of August and the trajectories show the prevailing northern airflow during the episode, resulting in elevated August levels of otherwise cleaner northern trajectories.

Clusters associated with the short trajectories need a further explanation. A side effect of trajectory clustering by using the Euclidean distance measure is grouping of short trajectories from different directions, because the Euclid-

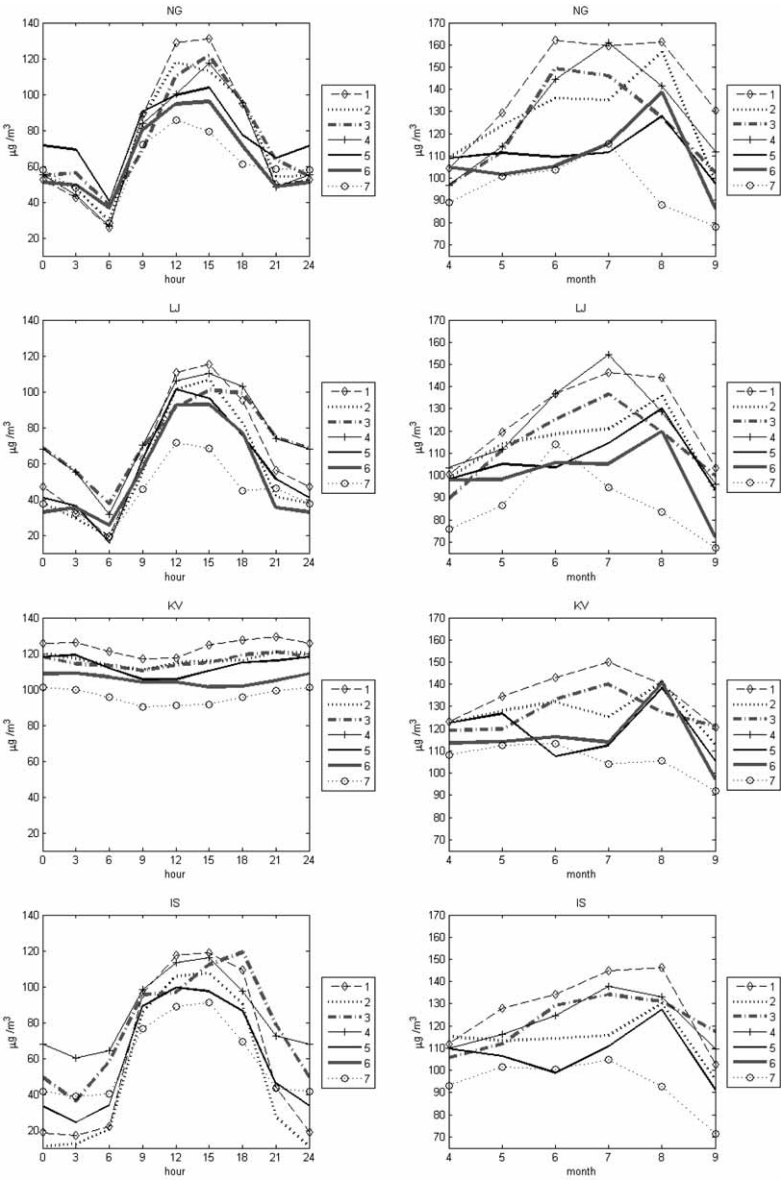

Figure 6. Analysis of average hourly ozone concentration clusters presented in Figure 4 for NG (first row), LJ (second row), KV (third row), and IS (fourth row). In the left panel, average diurnal ozone variations in clusters for months April–September are calculated from all trajectories and associated measured ozone values. Hours in left panel measure state UTC time. In the right panel, average cluster daily ozone maxima are associated with trajectories arriving at 12:00 and 15:00 UTC and averaged over all cluster 12:00 and 15:00 UTC trajectories. For KV ozone was averaged over all cluster trajectories and associated ozone concentrations. The cluster numbers correspond to the cluster labels in Figure 4.

ean measure is more sensitive to differences in long trajectories. Short trajectories, although originating from different directions, usually represent similar synoptic situations – warm days with light winds, associated with stable anticyclonic situations. Since the highest ozone concentrations are connected with the short trajectories from the SW we decided to apply a second stage clustering to these short trajectories. The second stage clusters, called sub-clusters from hereafter, show (not presented here with a table or a Figure) that the approaching directions for these short trajectories are rather diverse, but in general differences in ozone between pairs of sub-clusters are minor. Only for NG, the highest average ozone maximum is clearly connected with the sub-cluster originating from the north Adriatic Sea and reaching NG from the Gulf of Trieste. In this cluster also the absolute maximum hourly ozone concentration was measured 240 $\mu g/m^3$. The rather high ozone concentrations can be explained by local emission sources along that path. Some very high ozone values (above 180 $\mu g/m^3$) were measured also in other sub-clusters. But there is one sub-cluster originating directly from the Po Basin, with a much lower median, indicating less frequent occurrence of high ozone in this cluster. This result is opposing the idea that the precursors for high ozone concentrations originate directly from the Po Valley. Our results of second stage clustering for NG suggest that high ozone concentrations are in first place due to northward advection of polluted air masses, probably spread over the entire north Adriatic Sea or perhaps due to local sources of precursors along the northern part of the eastern Adriatic coastline. Emission sources over the Adriatic Sea itself are rare, so the pollutants were previously accumulated in the air – to some extent probably also over northern Italy (eventual indirect influence of the emissions from the Po Valley).

3.2. Concentration weighted trajectories and number density fields

A method of weighting trajectories with associated concentrations (CWT – see subsection 2.5) in combination with trajectory number density (ND) fields offers additional information about pathways of polluted air mass and potential source locations. Almost all NG polluted trajectories (Figure 7) travel over the north Adriatic Sea, over the Gulf of Trieste and reach NG from the south. There are some rare exceptions, namely trajectories originating either in northern Italy and reaching NG from the west, or originating in central Slovenia and reaching NG from the east. It must be also taken into account, that due to the local topography, southern flow toward Soča Valley north of NG usually develops in the fair weather conditions. The resulting trailing effect, where areas upwind and downwind of the sources are likely to be identified as sources as well, is eliminated in the CWT field, where the pattern at the Po River estuary indicates contribution of the Po Basin polluted air masses. The CWT field over the Adriatic Sea for NG is otherwise more or less homogeneous (except over the central Adriatic Sea, due to faster trajectories), and has noticeably higher values

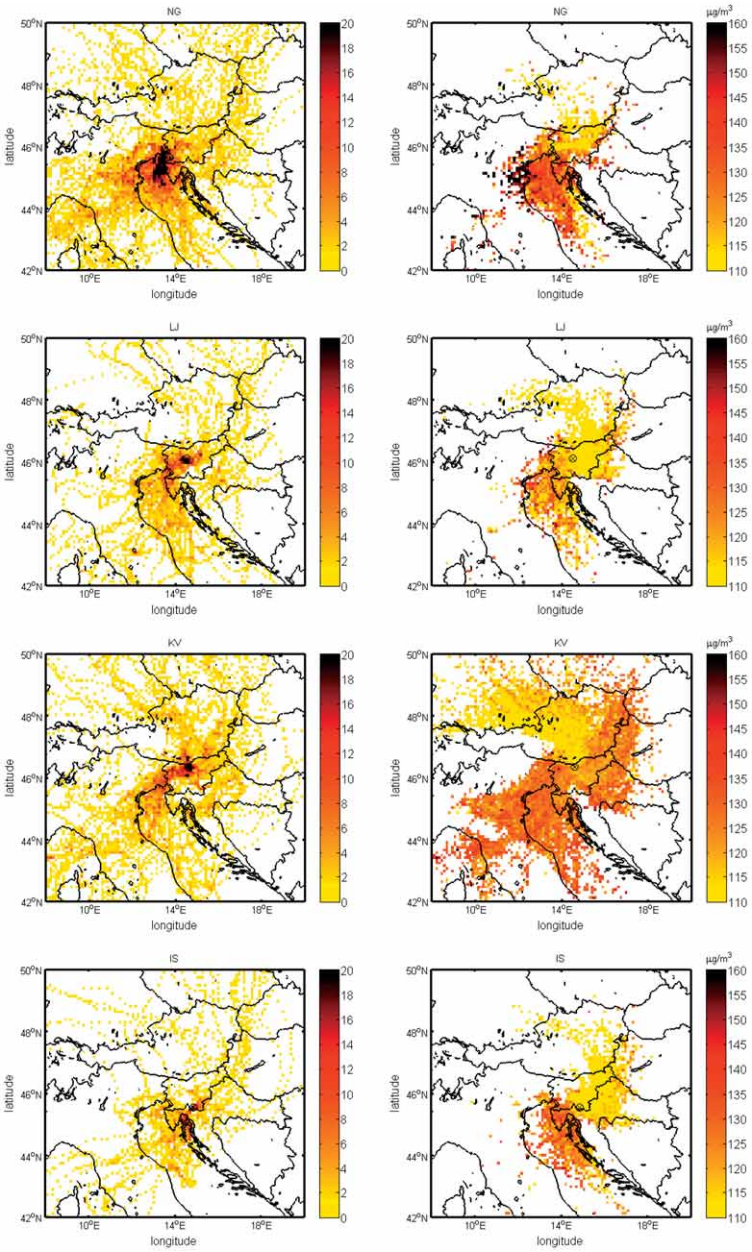

Figure 7. Analysis of 96-hour trajectories associated with 3h ozone maximum measured at receptor points NG, LJ, KV, and IS. Left panel: number density ND of trajectories with 3h ozone maximum above 160 μg/m^3. Right panel: CWT fields, where only grid values with at least 10 trajectory end points are presented (for NG, LJ, IS with at least 10 trajectory points in hours 12:00 – 15:00 UTC). Grid mesh has a resolution of 10 km.

than over Slovenia. Results are thus similar to conclusions of the cluster analysis. The highest ozone concentrations probably occur due to polluted air masses spread over the Mediterranean while a passage over emission areas in western Istria and the Gulf of Trieste enhances the total pollution.

Similar conclusions are valid for IS. ND for IS indicates that the most polluted air masses travel over the Gulf of Kvarner with industrial emission sources located on the coast and enhanced coastal traffic during the peak summer tourist season. Homogeneous CWT values over a broader coastal area and over the Adriatic Sea indicate that ozone polluted air masses are probably spread over a larger area south of Slovenia. The contribution of emissions located around Rijeka and surroundings most likely causes the final addition to the total ozone resulting in exceeding threshold values at the IS station.

The pollution accumulated in the Mediterranean air masses presents a contribution even for LJ, or rather a baseline, to which local emissions (which are probably dominant) are added. There are some »polluted« trajectories, approaching from the east, but the SW pattern of ND for LJ is prevalent. Similarly, the CWT field indicates cleaner NE trajectories towards LJ than SW trajectories.

Highly polluted air masses are always advected to KV. The most distinct ND pattern again occurs from the SW. In contrast to the other stations, there are three additional trails approaching from the N, NE and E, indicating that regional transport from Central and Eastern Europe is not always altogether negligible. The CWT values for KV are less variable. Regions over the north Adriatic Sea and northern Italy are associated with the highest CWT values, but the CWT values for eastern and northeastern flows are almost the same. Actually the only distinct pattern of CWT for KV is a significantly cleaner airflow of trajectories crossing the Alps and reaching the site from the north.

4. Conclusions

In the present paper, trajectory-based analysis has been applied to reveal the origins of ozone-polluted air masses for four measuring sites in Slovenia. Results of cluster analysis show that for all the stations the highest ozone concentrations are associated with southwesterly flow of air masses. For the high elevation station Krvavec (KV) the differences in ozone values for the short SW cluster compared to all other clusters are even statistically significant (*t*-test and Kruskal-Wallis test at 0.05 significance level). For the lower altitude stations ozone in the short SW cluster is significantly higher than in northern clusters (for LJ only according to *t*-test), while differences between several southern clusters are usually not significant.

The lowest measured ozone for all the stations is associated with the cluster of long NW trajectories, crossing the Alps and approaching Slovenia from the north. This »clean« air pathway is in great deal due to meteorological conditions, unfavorable for ozone formation.

Concentration weighted trajectories (CWT) in combination with number density (ND) of »polluted« trajectories indicated additional ozone-rich air path characteristics. The most interesting are the results for Nova Gorica (NG) and Iskrba (IS) with CWT patterns substantially higher over southern areas (the northern Adriatic Sea with its coastal regions), than over the rest of Slovenia. ND for each of the two sites reveals one very limited area, which is common to all »polluted trajectories«: the Gulf of Trieste, and the Gulf of Kvarner, for NG and IS, respectively. The possible conclusion for these two sites may be that very high ozone concentrations are in first place due to polluted air masses originating from the wider north Mediterranean area. While passing about 40 km distant coastal emission areas, the pollution is increased to the final values. The time, needed by air masses to travel the distance between the coastal areas and the two measuring sites, enable the photochemistry to take place and form ozone from its precursors.

The measuring site in the capital city Ljubljana (LJ) is strongly influenced by emissions from local traffic and some industrial sources. But even for LJ, the results of all analyses indicate the influence of polluted air masses originating from the SW.

Ozone characteristics of higher altitudes are reflected at Krvavec (KV). In addition to significant ozone contribution from the Mediterranean, CWT and ND patterns indicate trails of polluted air masses approaching from the N, NE, and E. These air masses predominantly originate from the Central Europe and usually travel around the eastern edge of the Alps before they reach Slovenia. A CWT field for KV suggests cleaner air masses originating again from the Central Europe, but now crossing the Alps and reaching KV from the north.

A significant influence of Central Europe pollution cannot be confirmed for NG, LJ and IS. There are only some rare northern trails in ND and CWT fields for those sites, suggesting that high ozone values are rarely associated with air masses originating from the north. The results as well did not confirm a direct pathway of polluted air from the Po River Basin to Slovenia, only the CWT field for NG shows a pattern toward the Po Basin. But still there may be a substantial indirect influence of this heavily industrialized area to the overall northern Mediterranean.

The stratospheric ozone intrusions were not the issue of the present research, but at least occasionally they may affect near ground ozone levels. Especially the elevated sites (like KV in Slovenia) are more exposed to this natural phenomenon (Schuepbach et al., 1999). For the urban areas elevated ozone concentrations due to intrusions from stratosphere are rare, but as well documented (e.g. Lisac et al., 1990; Klaić et al., 2003). The question remains whether the stratospheric intrusions should be somehow considered (filtered) in the presented trajectory analysis.

A common origin of ozone rich air masses for all stations and from all analysis results seems to be an area over the northern Adriatic Sea, which is rather unexpected. Since there are no significant precursor emissions (except

ships) over the sea, the coastal regions appear to be considerable source of ozone precursors. The northern Adriatic Sea was identified also by Kaiser et al. (2007) as a NO_x source for GAW stations and as an origin of ozone rich air masses for KV station. In addition, high ozone values measured at the coast in the northern Adriatic were reported by Cvitaš et al. (1997). This northern Adriatic Sea phenomenon needs further investigation. In the first place the ozone as well as other pollutant measurements over the sea is needed to establish the actual degree of photochemical pollution. Secondly, further research is required to identify which processes (different vertical mixing, deposition, etc.) are responsible for formation of the eventual polluted air masses over the sea and over the coastal areas.

The question whether the high ozone observations are primarily caused by transport of ozone or transport of ozone precursors, as well as the contribution of ozone formation from local emissions, remains difficult to answer only with the methodology applied. The trajectory analysis cannot take into account processes like chemical reactions, wet and dry deposition, and turbulence. To explain the ozone phenomenon over Slovenia, over the northern Adriatic Sea and its coastal regions accurately, all these processes must be considered. With the current approach we are therefore not in a position to evaluate for example the »indirect impact« of the Po Basin emissions relative to the more local emissions (i.e. the Gulfs of Trieste and Kvarner) on ozone in Slovenia. To find the answers to these questions, a photochemical model is required, left for the future research.

Acknowledgement – This research was supported by Ministry of Education, Science and Sport of the Republic of Slovenia (Grant L1-6709 and V4-0995). The authors would like to thank Mark Žagar from the Environmental Agency of the Republic of Slovenia for providing ALADIN meteorological fields and the same agency for all the measured data.

References

ALADIN International Team (2003). The ALADIN Project, mesoscale modeling seen as a basic tool for weather forecasting and atmospheric research, *WMO Bull.*, ***46,*** 317–324.

Abdalmogith, S. and Harrison, R. (2005): The use of trajectory cluster analysis to examine the long-range transport of secondary inorganic aerosol in the UK, *Atmos. Environ.*, ***39***, 6686–6695.

Avila, A. and Alarcon, M. (1999): Relationship between precipitation chemistry and meteorological situytions at a rural site in NE Spain, *Atmos. Environ.,* ***33***, 1663–1677.

Balzhanov, V. (1994): *Surface ozone at Mount Areskutan: Connection with ozone in the free troposphere, ITM report.* Stockholm.

Bizjak, M., Tursic, J., Lesnjak, M. and Cegnar, T. (1999): Aerosol black carbon and ozone measurements at Mt. Krvavec EMEP/GAW station, Slovenia, *Atmos. Environ.*, **33**, 2783–2787.

Black, E., Blackburn, M., Harrison, G., Hoskins, B. and Methven, J. (2004): Factors contributing to the summer 2003 European heatwave, *Weather*, **59**, 217–223.

Cape, J., Methven, J. and Hudson, L. (2000): The use of trajectory cluster analysis to interpret trace gas measurements at Mace Head, Ireland, *Atmos. Environ.,* **34**, 3651–3663.

Cristofanelli, P., Bonasoni, P., Carboni, G., Calzolari, F., Casarola, L., Sajani, S. et al. (2007): Anomalous high ozone concentrations recorded at a high mountain station in Italy in summer 2003, *Atmos. Environ.,* **41**, 1383–1394.

Cvitaš, T., Kezele, N., Klasinc, L. (1997): Boundary-Layer Ozone in Croatia, *J. Atmos. Chem.,* **28**, 125–134.

Derwent, R. and Davies, T. (1994): Modelling of the impact of NOx or hydrocarbon control on photochemical ozone in Europe, *Atmos. Environ.,* **28**, 2039–2052.

Derwent, R., Simmonds, P., Seuring, S. and Dimmer, C. (1998): Observation and interpretation of the seasonal cycles in the surface concentrations of ozone and carbon monoxide at Mace Head, Ireland from 1990 to 1994, *Atmos. Environ.,* **32**, 145–157.

Flemming, J., Stern, R. and Yamartino, R. (2005): A new air quality regime classification scheme for O3, NO2, SO2 and PM10 observation sites, *Atmos. Environ.,* **39**, 6121–6129.

Galvez, O. (2007): Synoptic-scale transport of ozone into Southern Ontario, *Atmos. Environ.,* **41**, 8579–8595.

Gibbons, J. (1985): *Nonparametric Statistical Inference, 2nd edition.* M. Dekker.

Gomišček, B., Cigler, R., Hrček, D., Gomišček, S., Lešnjak, M., Pauli, P. et al. (1997): Measurements of atmospheric constituents and their relationship to the ozone formation in Slovenia. In Hov, O. (Ed.): *Tropospheric ozone research,* Tropospheric ozone in the Regional and sub-regional context, Vol. 6. Berlin Heidelberg: Springer-Verlag, 271–276.

Gomišček, B., Cigler, R., Levart, A., Gomišček, S., Pauli, P., Baša, H. et al. (1997): The investigation of ozone atmospheric constituents related to ozone at two rural sites, *Acta Chim. Slov.*, **44**, 161–179.

Gomišček, B., Levart, A., Gomišček, S. and Duyzer, J. (1996): Dry deposition measurements of ozone overt a spruce forest in the Triglav National Park, Slovenia. *Proceedings of EUROTRAC Symposium '96*. Southampton: Computational Mechanics Publications, 325–329.

Hafner, W., Solorzano, N. and Jaffe, D. (2007): Analysis of rainfall and fine aerosol data using clustered trajectory analysis for National Park sites in the Western US, *Atmos. Environ.,* **41**, 3071–3081.

Harris, J., Draxler, R. and Oltmans, S. (2005): Trajectory model sensitivity to differences in input data and vertical transport method, *J. Geophys. Res.*, **110**, D14109.

Hochberg, Y. and Tamhane, A. (1987): *Multiple Comparison Procedures.* Wiley.

Hollander, M. and Wolfe, D. (1973): *Nonparametric Statistical Methods.* Wiley.

Kaiser, A., Scheinfinger, H., Spangl, W., Weiss, A., Gilge, S., Fricke, W., et al. (2007): Transport of nitrogen oxides, carbon monoxide and ozone to the Alpine Global Atmosphere Watch stations Jungfraujoch (Switzerland, Zugspitze and Hohenpeissenberg (Germany), Sonnblick (Austria) and Mt. Krvavec (Slovenia), *Atmos. Environ.*, **41**, 9273–9287.

Kim Oanh, N., Chutimon, P., Ekbordin, W. and Supat, W. (2005): Meteorological pattern classification and application for forecasting air pollution episode potential in a mountain-valley area, *Atmos. Environ.,* **39**, 1211–1225.

Klaić, Z. B., Belušić, D., Bulić, I.H., Hrust,L. (2003): Mesoscale modeling of meteorological conditions in the lower troposphere during a winter stratospheric ozone intrusion over Zagreb, Croatia, *J. Geophys. Res.*, **108**(D23), 4720, doi:10.1029/2003JD003878.

Lefohn, A., Shadwick, D., Feister, U. and Mohnen, V. (1992): Surface level ozone: climate change and evidence for trends, *J. Air Waste Manage.,* **42**, 136–144.

Lin, C., Cheng, M. and Schroeder, W. (2001): Transport patterns and potential sources of total gaseous mercury measured in Canadian high Arctic in 1995, *Atmos. Environ.,* **35**, 1141–1154.

Lisac, I., Marki, A., Tiljak, D., Klasinc, L., Cvitaš, T. (1993): Stratospheric ozone intrusion over Zagreb, Croatia, on February 6, 1990., *Meteorol. Z.*, **2**, 224–231.

Logan, J. (1989): Ozone in rural areas of the United States, *J. Geophys. Res.,* **94**, 8511–8532.

Logan, J. (1985): Tropospheric ozone: seasonal behaviour, trends, and anthropogenic influence, *J. Geophys. Res.*, 10463–10482.

Mahura, A., Jaffe, D., Andres, R. and Merrill, J. (1999): Atmospheric transport pathways from the Bilibino nuclear power plant to Alaska, *Atmos. Environ.,* ***33***, 5115–5122.

Makra, L., Mika, J., Bartzokas, A., Beczi, R., Borsos, E. and Suemeghy, Z. (2006): An objective classification system of air mass types for Szeged Hungary, with special interest in air pollution levels, *Meteorol. Atmos. Phys.,* **92**, 115–137.

Monks, S. (2000): A review of the observations and origins of the spring ozone maximum, *Atmos. Environ.,* **34**, 3454–3561.

Moody, J. and Galloway, J. (1988): Quantifying the relationship between atmospheric transport and the chemical composition of precipitation on Bermuda, *Tellus,* **40B**, 436–479.

Ordonez, C., Mathis, H., Furger, M., Henne, S., Hungin, C., Staehelin, J. et al. (2005): Changes of daily surface ozone maxima in Switzerland in all seasons from 1992 to 2002 and discussion of summer 2003, *Atmos. Chem. Phys.,* **5**, 1187–1203.

Owen, R. (2003): *A Climatological Study of Transport to the PICO-NARE Site Using Atmospheric Backward Trajectories, Civil and Environmental Engineering,* Michigan Technological University, Master of Science. Houghton.

Pilegaard, K., Skiba, U., Ambus, P., Beier, C., Brueggermann, N., Bahl-Butterbach, K. et al. (2006): The Millan photooxidant plume, *J. Geophys. Res.*, 23375–23388.

Prevot, A., Staehelin, J., Kok, G., Schillawski, R., Neininger, B., Staffelbach, T. et al. (1997): Factors controlling regional differences in forest soil emission of nitrogen oxides (NO and N_2O), *Biogeosciences*, **3**, 651–661.

Ricco, A., Giunta, G. and Chianese, E. (2007): The application of a trajectory classification procedure to interpret air pollution measurements in the urban area of Naples (Southern Italy), *Sci. Total Environ.*, **376**, 198–214.

Rousseaw, P. (1987): A graphical aid to the interpretation and validation of cluster analysis, *J. Comput. Appl. Math.*, **20**, 53–65.

Sanchez-Ccoyllo, O., Silva Diaz, P., Andrade, M. and Freitas, S. (2006): Determination of O3, Co and PM10 transport in the metropolitan area of Sao Paulo, Brazil through synoptic-scale analysis of back trajectories, *Meteorol. Atmos. Phys.*, **92**, 83–93.

Schaer, C. and Jendritzky, G. (2004): Hot news from summer 2003, *Nature*, **432**, 559–560.

Scheel, H., Areskoug, H., Geiss, H., Gomiscek, B., Granby, K., Haszpra, L., et al. (1997): On the spatial Distribution and seasonal variation of lower-troposphere ozone over Europe, *J. Atmos. Chem.*, **28**, 11–28.

Seibert, P., Frank, A. and Formayer, H. (2007): Synoptic and regional patterns of heavy precipitation in Austria, *Theor. Appl. Climatol.*, **87**, 139–153.

Seibert, P., Kromp-Kolb, H., Baltensperger, U., Jost, D., Schwinkowski, M., Kasper, A. et al. (1994): Trajectory analysis of aerosol measurements at high Alpine sites. *Transport and transformation of pollutants in the troposphere*, Den Haag: Academic Publishing, 689–693.

Seibert, P., Kromp-Kolb, H., Kasper, A., Kalina, M., Puxbaum, M., Jost, D. et al. (1997): Transport of polluted boundary layer air from the Po Valley to high Alpine sites, *Atmos. Environ.*, 3953–3965.

Schuepbach, E., Davies, T. D., Massacand, A. C. (1999): An unusual springtime ozone episode at high elevation in the Swiss Alps: Contribution both from cross-tropopause exchange and from the boundary layer, *Atmos. Environ.*, **33**, 1735 – 1744.

Stohl, A. and Seibert, P. (1998): Accuracy of trajectories as determined from the conservation of meteorological tracers, *Q. J. Roy. Met. Soc.*, **124**, 1465–1484.

Stohl, A., Wotawa, G., Seibert, P. and Kromp-Kolb, H. (1995): Interpolation errors in wind fields as a function of spatial and temporal resotluion and their impact on different types of kinematic trajectories, *J. Appl. Meteorol.*, **34**, 2149–2165.

Vautard, R., Honore, C., Beekmann, M. and Rouil, L. (2005): Simulation of ozone duringthe August 2003 heat wave and emission control scenarion, *Atmos. Environ.,* **39**, 2957–2967.

Wotawa, G. and Kromp-Kolb, H. (2000): The research project VOTALP – general objectives and main results, *Atmos. Environ.*, 1319–1322.

Wotawa, G., Kroeger, H. and Stohl, A. (2000): Transport of ozone towards the Alps – result from trajectory analyses and photochemical model studies, *Atmos. Environ.*, 1367–1377.

SAŽETAK

Analiza trajektorija onečišćenja ozona u Sloveniji

Rahela Žabkar, Jože Rakovec i Saša Gaberšek

Godišnji broj dana s vrijednostima većim od graničnih na postajama za kakvoću zraka u Sloveniji kreće se od nekoliko dana u unutrašnjosti pa sve do 25 dana na postajama Mediterana. Najveći broj slučajeva povećanja ozona je zabilježen u jugozapadnom dijelu Slovenije, blizu Jadrana, gdje odgovarajući meteorološki uvjeti povećavaju stvaranje ozona. Lokalni izvori onečišćenja u ovom dijelu zemlje ne mogu objasniti mjereni nivo onečišćenja. Također, visoke koncentracije ozona su povremeno mjerene i na ruralnim postajama u Sloveniji. Izveli smo analizu ozona u odnosu na porijeklo zračnih masa koja nam je omogućila uvid u procese koji vode prema visoko mjerenim koncentracijama prizemnog ozona. Izračunate su trodimenzionalne trajektorije s 3-satnim vremenskim intervalom unatrag za 4 mjerne postaje u Sloveniji, generirajući vremena dolaska po danu počevši u 00:00 UTC, za topli dio (travanj – rujan) 2003. i 2004. godine. Korišteno je grupiranje trajektorija radi određivanja tipičnih staza zračnih masa. Dalje su se analizirali ozon i osnovne meteorološke karakteristike grupa trajektorija te su primijenjeni višestruki testovi usporedbe radi određivanja koji se par klastera razlikuje značajnije u mjerenom ozonu. Kao dodatak su izračunate otežane trajektorije koncentracija (CWT) i broj gustoće (ND) »trajektorija onečišćenja« radi dobivanja dodatnih informacija o mogućim regionalnim izvorima emisije.

Rezultati sugeriraju da se visoke koncentracije ozona pojavljuju najčešće u klasterima kratkih trajektorija sporo-gibajućih jugozapadnih zračnih masa. Nadalje, CWT i ND polja potvrđuju da su visoke vrijednosti prizemnog ozona u Sloveniji uobičajeno povezane s trajektorijama koje potječu sa sjevernog dijela Jadrana i njegove obalne zone. Izrazito industrijalizirano područje bazena rijeke Po nema značajniji direktni utjecaj na mjerene koncentracije ozona u Sloveniji, ali može znatno doprinijeti sveukupnom onečišćenju nad sjevernim Jadranom zajedno s obalnim emisijama.

Ključne riječi: troposferski ozon, trajektorije, grupiranje, transport

Corresponding author's address: R. Žabkar, University of Ljubljana, Faculty of Mathematics and Physics, Chair of Meteorology, Jadranska 19, 1410 Ljubljana, Slovenia, tel: 00386–1–4766–639, e-mail: rahela.zabkar@fmf.uni-lj.si